Electronic Supplementary Information

Experimental section

Materials: sodium sulfide (Na_2S), sodium sulfate (Na_2SO_4), ammonium chloride (NH_4Cl), anhydrous lithium perchlorate ($LiClO_4$), hydrazine hydrate ($N_2H_4{\cdot}H_2O$), sodium hypochlorite (NaClO), sodium hydroxide (NaOH), sodium salicylate ($C_7H_5O_3Na$), ethanol (CH_3CH_2OH), and carbon paper were bought from Beijing Chemical Corporation. Para-(dimethylamino) benzaldehyde ($C_9H_{11}NO$), sodium nitroferricyanide (III) dihydrate ($Na_2Fe(CN)_5NO{\cdot}2H_2O$), and Nafion were purchased from Aladdin Ltd. (Shanghai, China). The water used throughout all experiments was purified through a Millipore system.

Preparation of S, EG, and SDG: Graphene was prepared from graphite rods by using electrochemical exfoliation which was performed in a two-electrode system. To prepare S and SDG， the titanium mesh and graphite rod were used as working anode, respectively, and the graphite rod as the counter electrode. The distance between the electrodes was 2 ± 0.5 cm and was kept constant throughout the electrochemical process. The electrolyte for the deposition was prepared by dispersing Na_2SO_4 (0.05 M, 0.710 g) and Na_2S (1.20 g) in 100 mL of DI water. For comparison, EG was also prepared by same method of SDG except the addition of Na_2S.

Pretreatment of titanium mesh and graphite rods: The titanium mesh was placed in a beaker containing a certain amount of concentrated hydrochloric acid and heated in an oil bath (100 ℃). The heating was stopped after the hydrochloric acid boiled for five minutes. Graphite rods were directly put into the ultrasonic machine for 30 minutes.

Preparation of S/CP, EG/CP, SDG/CP: Carbon paper (CP) was cleaned via brief sonication with ethanol and water for several times. 10 mg sample and 40 μL 5 wt% Nafion solution were dispersed in 960 μL water/ethanol (V : V = 1 : 3) followed by 1-h sonication to form a homogeneous ink. 20 μL ink was loaded onto a CP (1×1 cm^2) and dried under ambient condition.

Characterizations: XRD patterns were obtained from a Shimazu XRD-6100 diffractometer with Cu Kα radiation (40 kV, 30 mA) of wavelength 0.154 nm (Japan). SEM images were collected from the tungsten lamp-equipped SU3500 scanning electron microscope at an accelerating voltage of 20 kV (HITACHI, Japan). TEM images were obtained from a Zeiss Libra 200FE transmission electron microscope operated at 200 kV. XPS measurements were performed on an ESCALABMK II X-ray photoelectron spectrometer using Mg as the exciting source. The absorbance data of spectrophotometer were measured on SHIMADZU UV-1800 ultraviolet-visible (UV-Vis) spectrophotometer. The ion chromatography data were collected on Thermofisher ICS 5000 plus using the dual temperature heater, injection valve, conductivity detector, AERS 500 Anions suppressor.

Electrochemical measurements: Electrochemical measurements were performed with a CHI 660E electrochemical analyzer (CH Instruments, Inc., Shanghai) using a standard three-electrode system using SDG/CP as the working electrode, graphite rod as the counter electrode, and saturated Ag/AgCl electrode as the reference electrode. In all measurements, saturated Ag/AgCl electrode was calibrated with respect to reversible hydrogen electrode as following: in 0.5 M $LiClO_4$ aqueous solution, $E(RHE) = E(Ag/AgCl) + 0.059 \times pH + 0.197$ V. All experiments were carried out at room temperature. For N_2 reduction experiments, the 0.5 M $LiClO_4$ electrolyte was purged with N_2 for 30 min before the measurement. Potentiostatic test was conducted in N_2-saturated 0.5 M $LiClO_4$ solution in a two-compartment cell, which was separated by Nafion 117 membrane.

Determination of NH_3: The produced NH_3 was detected with indophenol blue by ultraviolet spectroscopy[1] and ion chromatography.[2] For the ultraviolet spectroscopy, 4 mL electrolyte was obatined from the cathodic chamber and mixed with 50 μL oxidizing solution containing NaClO ($\rho Cl = 4 \sim 4.9$) and NaOH (0.75 M), 500 μL coloring solution containing 0.4 M $C_7H_6O_3Na$ and 0.32 M NaOH, and 50 μL catalyst solution (1 wt% $Na_2[Fe(CN)_5NO]$) for 1 h. Absorbance measurements were performed at $\lambda = 655$ nm. The concentration-absorbance curve was calibrated using standard NH_4^+ solution with a serious of concentrations. The fitting curve ($y = 0.353x$

+ 0.009, R^2 = 0.999) shows good linear relation of absorbance value with NH_4^+ concentration.

Determination of N_2H_4: The N_2H_4 present in the electrolyte was determined by the method of Watt and Chrisp.[3] The mixture of $C_9H_{11}NO$ (5.99 g), HCl (30 mL), and C_2H_5OH (300 mL) was used as a color reagent. In detail, 5 mL electrolyte was removed from the electrochemical reaction vessel, and added into 5 mL above prepared color reagent and stirring 10 min at room temperature. Moreover, the absorbance of the resulting solution was measured at a wavelength of 460 nm. The concentration absorbance curves were calibrated using standard N_2H_4 solution with a series of concentrations. The fitting curve ($y = 0.627x + 0.047$, $R^2 = 0.999$) shows good linear relation of absorbance value with N_2H_4 concentration.

Calculations of NH_3 yield and FE: NH_3 yield was calculated using the following equation:

$$NH_3 \text{ yield} = [NH_4^+] \times V/(m_{cat.} \times t)$$

FE was calculated according to following equation:

$$FE = 3 \times F \times [NH_4^+] \times V/(18 \times Q)$$

Where $[NH_4^+]$ is the measured NH_4^+ concentration; V is the volume of the cathodic reaction electrolyte; t is the potential applied time; $m_{cat.}$ is the loaded quality of catalyst; F is the Faraday constant; and Q is the quantity of charge in Coulombs.

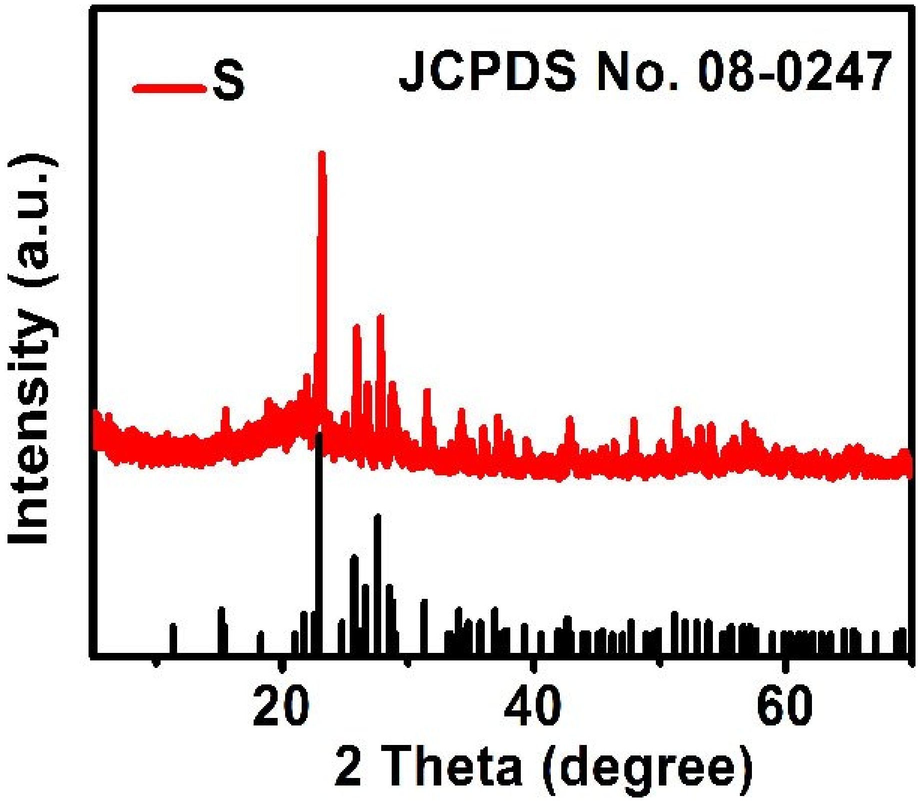

Fig. S1. XRD pattern of S.

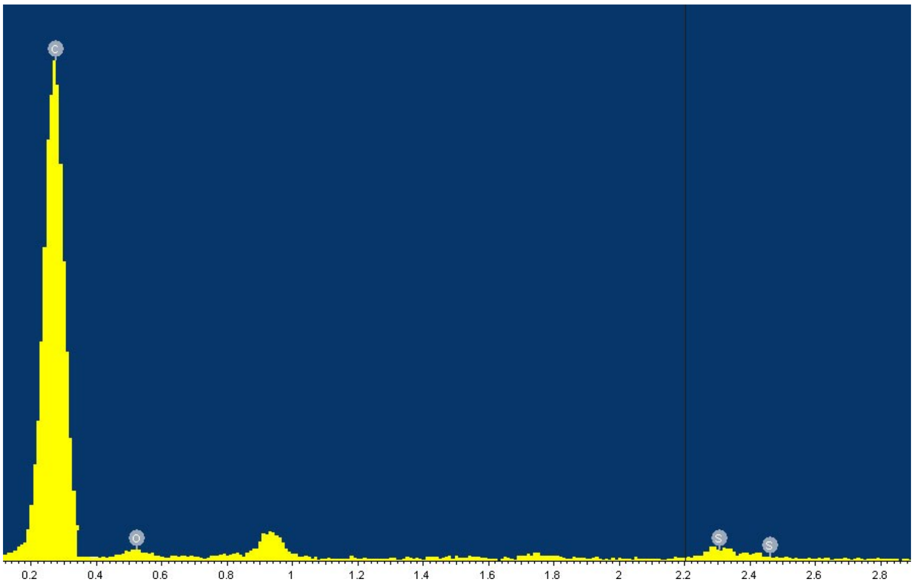

Fig. S2. EDX spectrum of SDG.

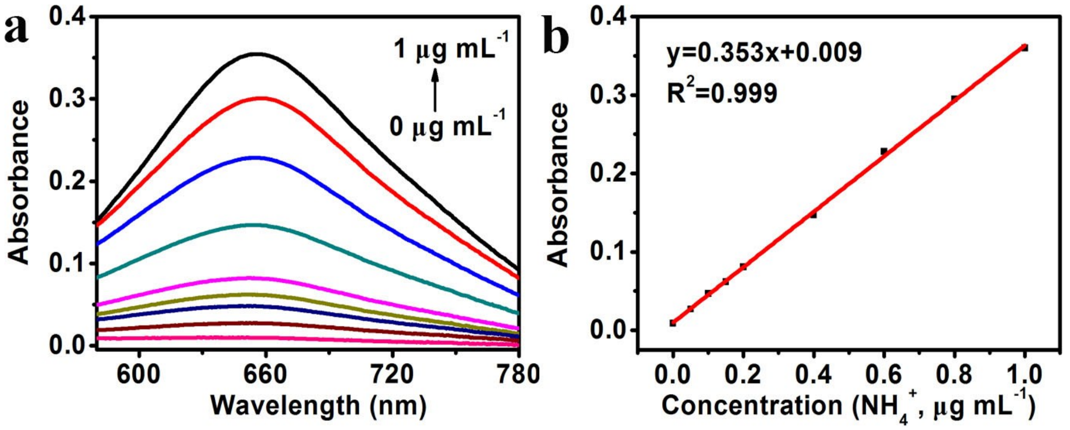

Fig. S3. (a) UV-Vis absorption spectra of indophenol assays with NH_4^+ concentrations after incubated for 2 h at room temperature. (b) Calibration curve used for calculation of NH_4^+ concentrations.

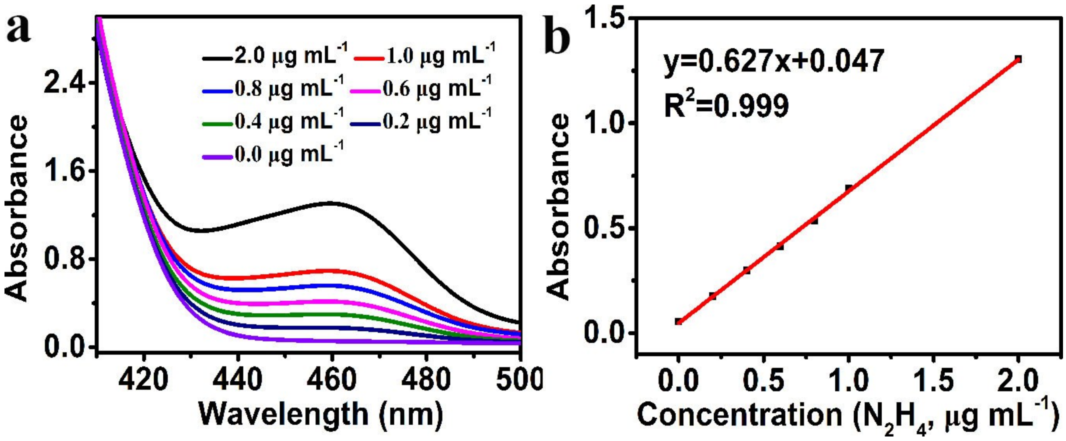

Fig. S4. (a) UV-Vis absorption spectra of various N_2H_4 concentrations after incubated for 10 min at room temperature. (b) Calibration curve used for calculation of N_2H_4 concentrations.

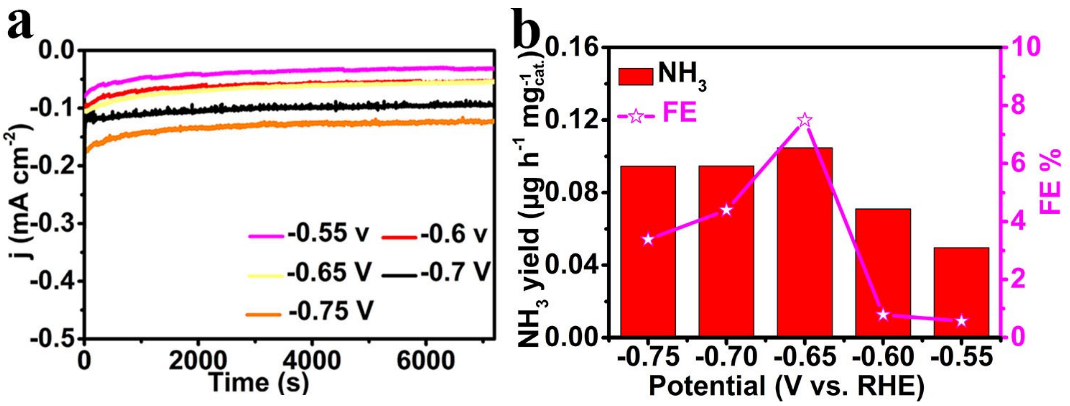

Fig. S5. (a) Time-dependent current density curves for SDG/CP at different potentials in 0.1 M Na_2SO_4. (b) NH_3 yields and FEs for SDG/CP at a series of potential.

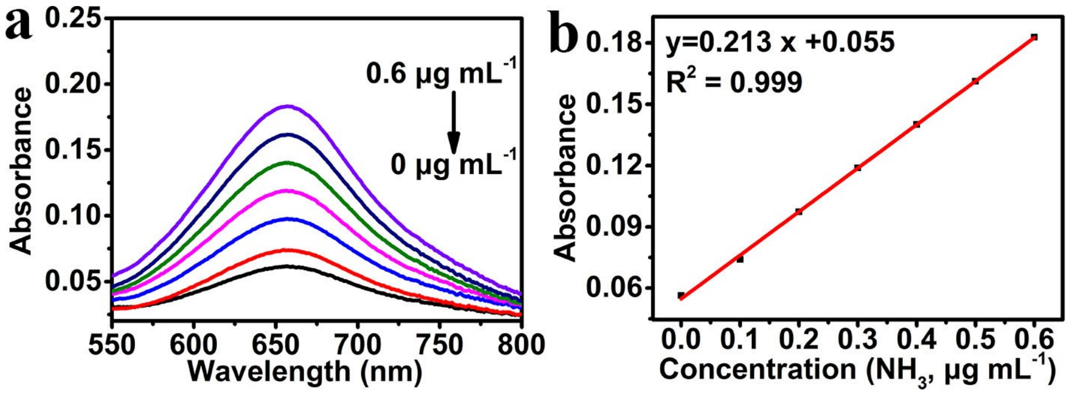

Fig. S6. (a) UV-Vis curves of indophenol assays with NH_4^+ ions in 0.1 M HCl after incubated for 2 h at room temperature. (b) Calibration curve used for calculation of NH_3 concentrations in 0.1 M HCl.

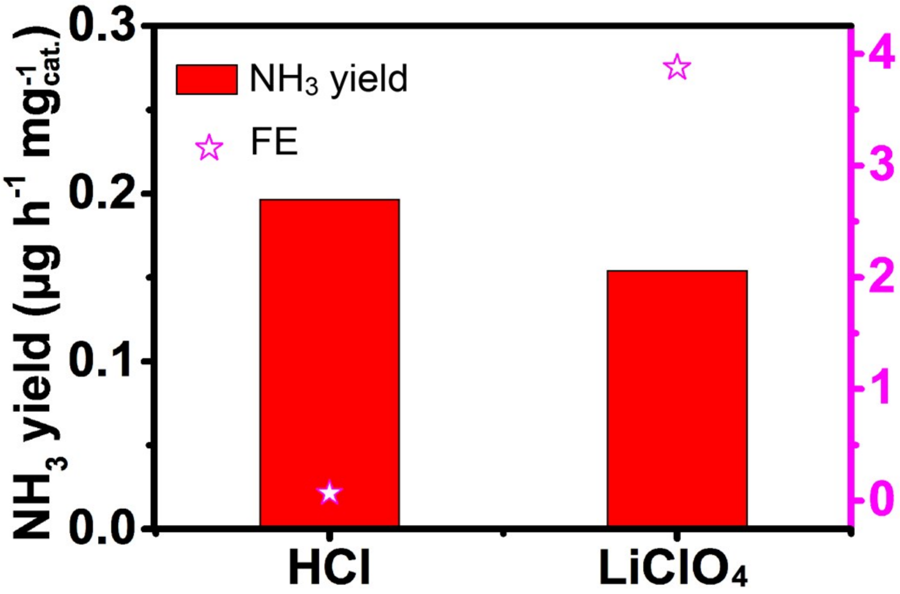

Fig. S7. NH_3 yields and FEs of SDG/CP in 0.1 M HCl and 0.1 M $LiClO_4$ at -0.85 V.

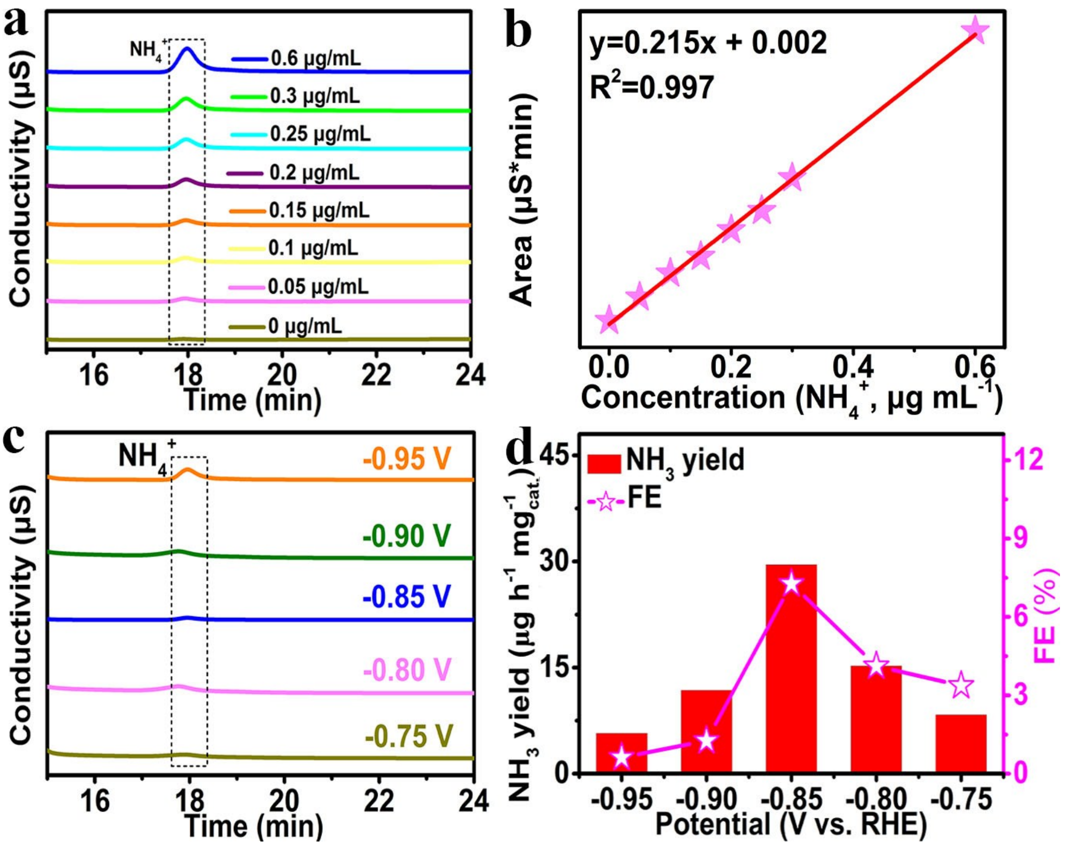

Fig. S8. (a) Ion chromatogram for the standard NH_4^+ samples and (b) corresponding calibration curve. (c) Ion chromatogram for the electrolytes at a series of potentials after electrolysis for 2 h. (d) NH_3 yields and FEs for SDG/CP at corresponding potentials.

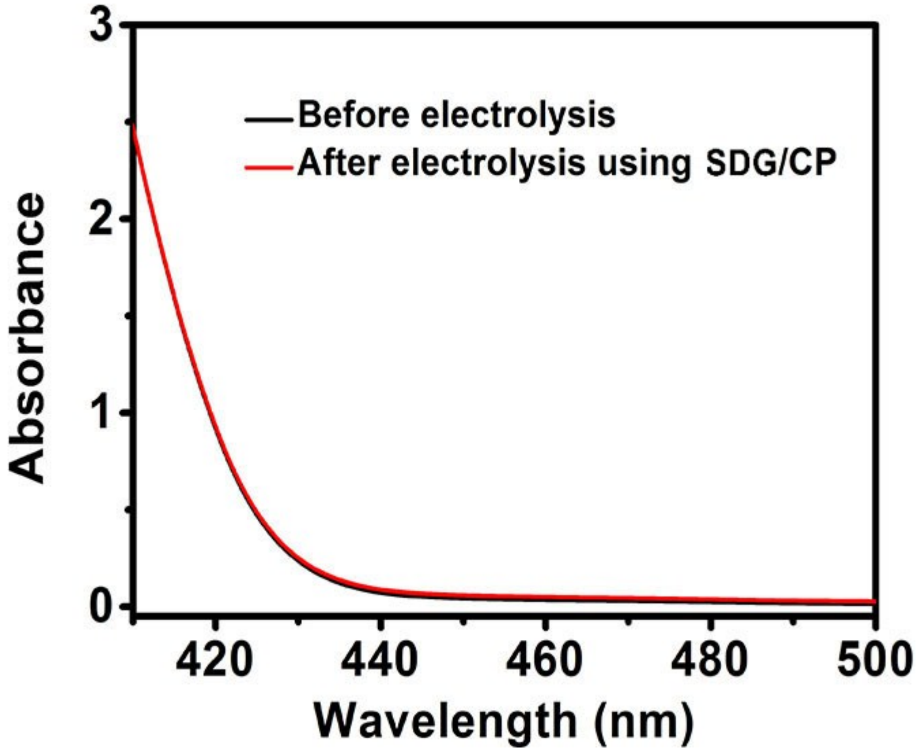

Fig. S9. UV-Vis absorption spectra of electrolytes stained with para-(dimethylamino) benzaldehyde indicator before and after 2 h electrolysis.

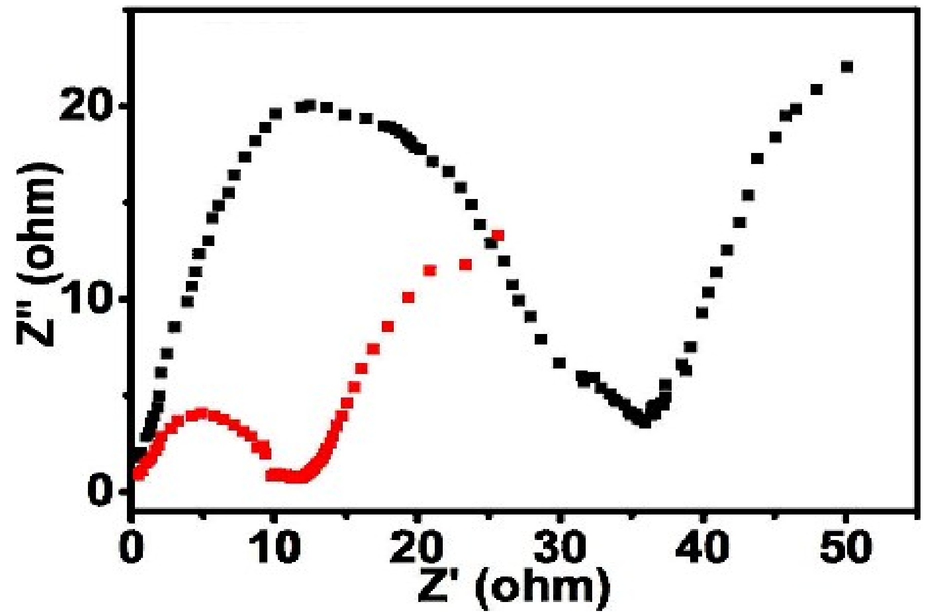

Fig. S10. Nyquist plots of SDG/CP (red curve) and S/CP (black curve).

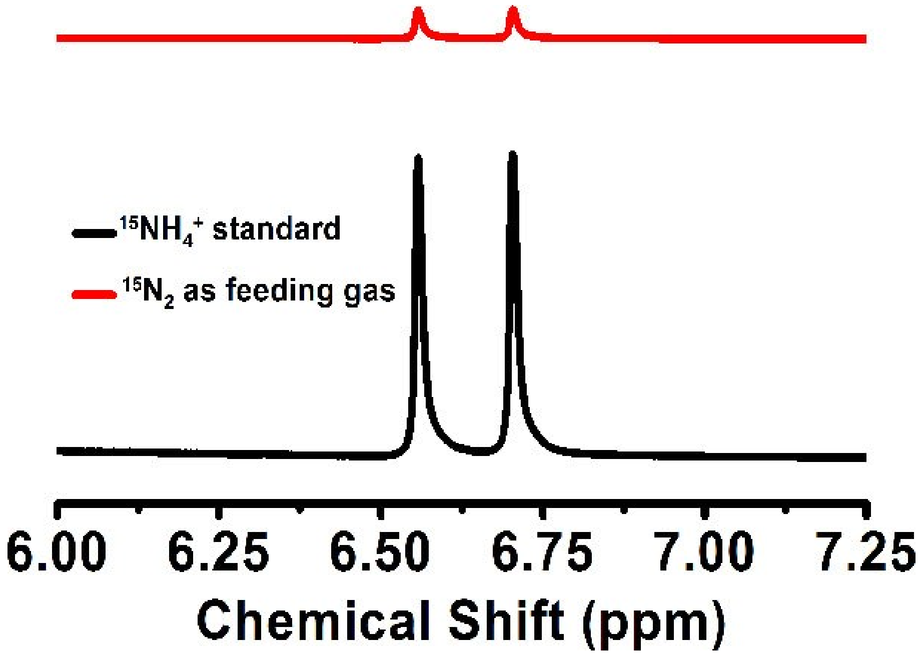

Fig. S11. ^1H NMR spectra of $^{15}NH_4^+$ standand sample and the product obtained after electrolysis at –0.85 V under $^{15}N_2$ atmosphere on the SDG/CP.

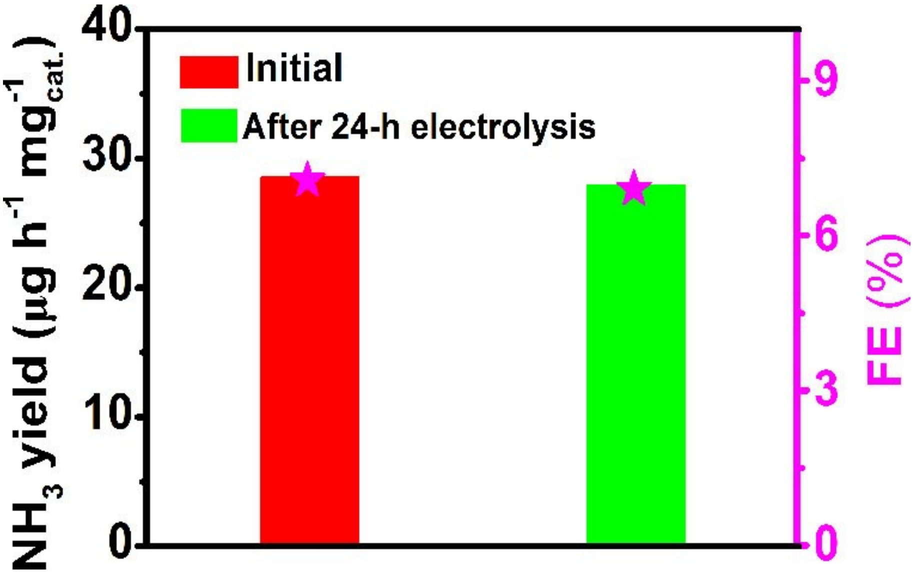

Fig. S12. NH_3 yields and FEs after charging at –0.85 V for 2 and 24 h.

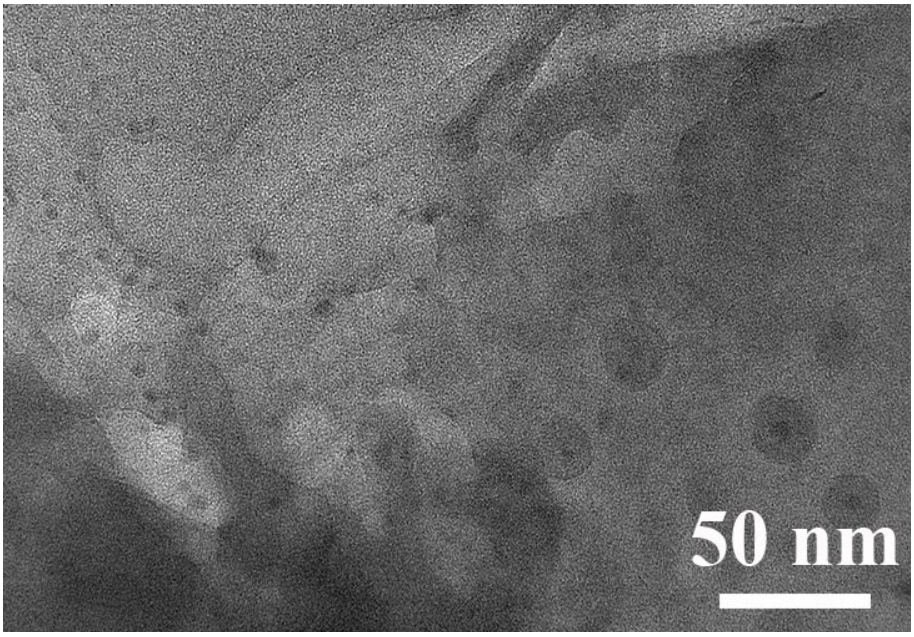

Fig. S13. TEM image of SDG after stability test.

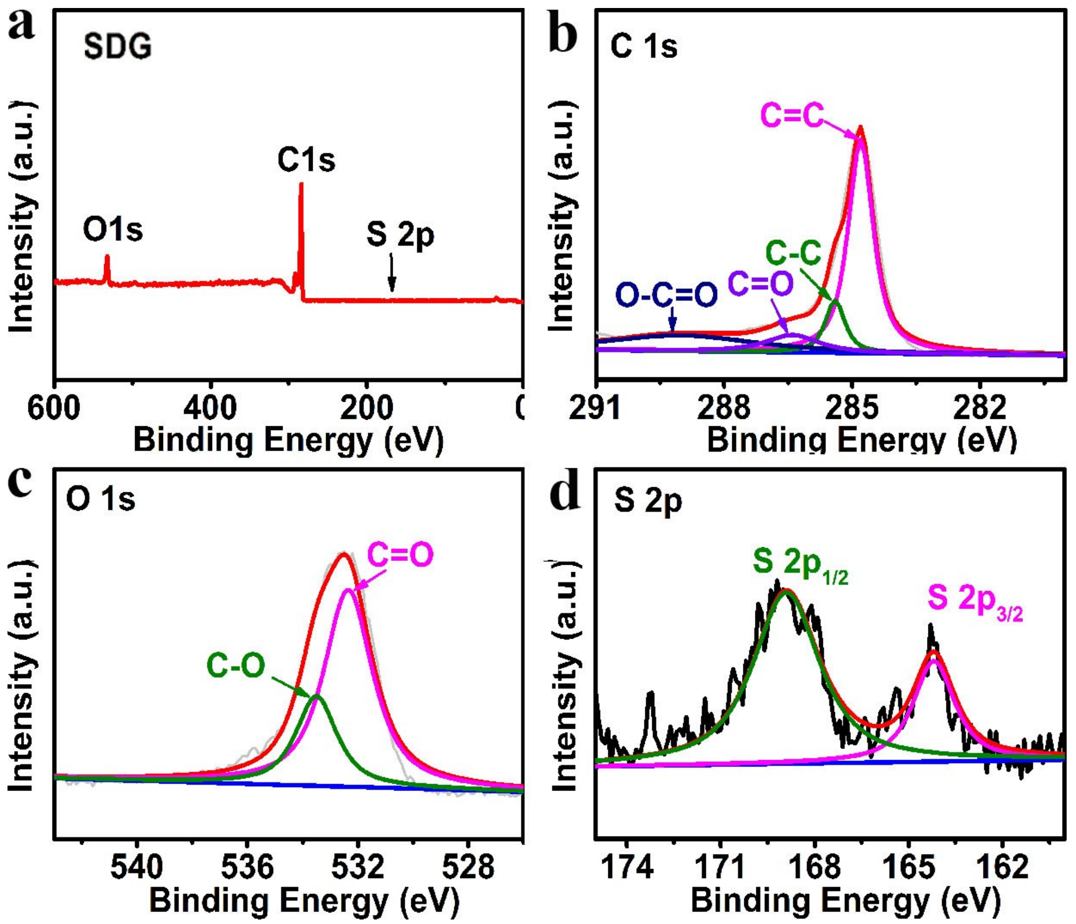

Fig. S14. XPS spectra of SDG after NRR test in the (a) SDG, (b) C 1s, (c) O 1s and (d) S 2p regions.

Table S1. Comparison of the electrocatalytic NRR performance of SDG with other NRR electrocatalysts under ambient reaction conditions in aqueous media.

Catalyst	**Electrolyte**	**NH_3 yield**	**FE(%)**	**Ref.**
SDG	0.5 M $LiClO_4$	28.56 μg h^{-1} $mg^{-1}_{cat.}$	7.07	This work
PEBCD/C	0.5 M Li_2SO_4	1.58 μg h^{-1} cm^{-2}	2.85	4
β-FeOOH nanorod	0.5 M $LiClO_4$	23.32 μg h^{-1} $mg^{-1}_{cat.}$	6.7	5
CNS	0.25 M $LiClO_4$	97.18 μg h^{-1} cm^{-2}	11.56	6
MoS_2/CC	0.1 M Na_2SO_4	8.8×10^{-11} mol s^{-1} cm^{-2}	1.17	7
Fe_3O_4/Ti	0.1 M Na_2SO_4	5.6×10^{-10} mol s^{-1} cm^{-2}	2.6	8
Mn_3O_4 nanocube	0.1 M Na_2SO_4	11.6 μg h^{-1} $mg^{-1}_{cat\cdot}$	3.0	9
TiO_2-rGO	0.1 M Na_2SO_4	15.13 μg h^{-1} $mg^{-1}_{cat.}$	3.3	10
B-TiO_2	0.1 M Na_2SO_4	14.4 μg h^{-1} $mg^{-1}_{cat.}$	3.4	11
C-TiO_2	0.1 M Na_2SO_4	16.22μg h^{-1} $mg^{-1}_{cat.}$	1.84	12
VO_2 hollow microsphere	0.1 M Na_2SO_4	14.85 μg h^{-1} $mg^{-1}_{cat.}$	3.97	13
hollow Cr_2O_3 microspheres	0.1 M Na_2SO_4	25.3 μg h^{-1} $mg^{-1}_{cat.}$	6.78	14
Fe_2O_3 nanorods	0.1 M Na_2SO_4	15.9 μg h^{-1} $mg^{-1}_{cat.}$	0.94	15
MnO	0.1 M Na_2SO_4	1.11×10^{-10} mol s^{-1} cm^{-2}	8.02	16
Mn_3O_4 nanocube	0.1 M Na_2SO_4	11.6 μg h^{-1} $mg^{-1}_{cat.}$	3.0	17
N-doped porous carbon	0.05 M H_2SO_4	1.40 mmol g^{-1} h^{-1}	1.42	18
polymeric carbon nitride	0.1 M HCl	8.09 μg h^{-1} $mg^{-1}_{cat.}$	11.59	19
B_4C nanosheet	0.1 M HCl	26.57 μg h^{-1} $mg^{-1}_{cat.}$	15.95	20
Black P nanosheet	0.01 M HCl	31.37 μg h^{-1} $mg^{-1}_{cat.}$	5.07	21

References

1 D. Zhu, L. Zhang, R. E. Ruther and R. J. Hamers, *Nat. Mater.*, 2013, **12**, 836–841.

2 J. Weiss, *Handbook of Ion Chromatography,* John Wiley & Sons, 2016, **2**.

3 G. W. Watt and J. D. Chrisp, *Anal. Chem.*, 1952, **24**, 2006–2008

4 G. Chen, X. Cao, S. Wu, X. Zeng, L. Ding, M. Zhu and H. Wang, *J. Am. Chem. Soc.*, 2017, **139**, 9771–9774.

5 X. Zhu, Z. Liu, Q. Liu, Y. Luo, X. Shi, A. M. Asiri, Y. Wu and X. Sun, *Chem. Commun.*, 2018, **54**, 11332–11335.

6 Y. Song, D. Johnson, R. Peng, D. K. Hensley, P. V. Bonnesen, L. Liang, J. Huang, F. Yang, F. Zhang, R. Qiao, A. P. Baddorf, T. J. Tschaplinski, N. L. Engle, M. C. Hatzell, Z. Wu, D. A. Cullen, H. M. Meyer III, B. G. Sumpter and A. J. Rondinone, *Sci. Adv*., 2018, **4**, e1700336.

7 L. Zhang, X. Ji, X. Ren, Y. Ma, X. Shi, Z. Tian, A. M. Asiri, L. Chen, B. Tang and X. Sun, *Adv. Mater.* 2018, **30**, 1800191.

8 Q. Liu, X. Zhang, B. Zhang, Y. Luo, G. Cui, F. Xie and X. Sun, *Nanoscale*, 2018, **10**, 14386–14389.

9 X. Wu, L. Xia, Y. Wang, W. Lu, Q. Liu, X. Shi and X. Sun, *Small*, 2018, **14**, 1803111.

10 X. Zhang, Q. Liu, X. Shi, A. M. Asiri, Y. Luo, X. Sun and T. Li, *J. Mater. Chem. A*, 2018, **6**, 17303–17306.

11 Y. Wang, K. Jia, Q. Pan, Y. Xu, Q. Liu, G. Cui, X. Guo and X. Sun, *ACS Sustainable Chem. Eng.*, 2019, **7**, 117–122.

12 K. Jia, Y. Wang, Q. Pan, B. Zhong, Y. Luo, G. Cui, X. Guo and X. Sun, *Nanoscale Adv.*, 2019, DOI: 10.1039/c8na00300a.

13 R. Zhang, H. Guo, L. Yang, Y. Wang, Z. Niu, H. Huang, H. Chen, L. Xia, T. Li, X. Shi, X. Sun, B. Li and Q. Liu, *ChemElectroChem.*, 2018, DOI: 10.1002/celc.201801484.

14 Y. Zhang, W. Qiu, Y. Ma, Y. Luo, Z. Tian, G. Cui, F. Xie, L. Chen, T. Li and X. Sun, *ACS Catal.*, 2018, **8**, 8540–8544.

15 X. Xiang, Z. Wang, X. Shi, M. Fan and X. Sun, *ChemCatChem*, 2018, **10**, 1–7.

16 Z. Wang, F. Gong, L. Zhang, R. Wang, L. Ji, Q. Liu, Y. Luo, H. Guo, Y. Li, P. Gao, X. Shi, B. Li, B. Tang and X. Sun, *Adv. Sci.*, 2018, **5**, 1801182.

17 X. Wu, L. Xia, Y. Wang, W. Lu, Q. Liu, X. Shi and X. Sun, *Small*, 2018, **14**, 1803111.

18 Y. Liu, Y. Su, X. Quan, X. Fan, S. Chen, H. Yu, H. Zhao, Y. Zhang and J. Zhao, *ACS Catal.*, 2018, **8**, 1186–1191.

19 C. Lv, Y. Qian, C. Yan, Y. Ding, Y. Liu, G. Chen and G. Yu, *Angew. Chem., Int. Ed.*, 2018, **57**, 10246–10250.

20 W. Qiu, X. Xie, J. Qiu, W. Fang, R. Liang, X. Ren, X. Ji, G. Cui, A. M. Asiri, G. Cui, B. Tang and X. Sun, *Nat. Commun.*, 2018, **9**, 3485.

21 L. Zhang, L. Ding, G. Chen, X. Yang and H. Wang, *Angew. Chem., Int. Ed.*, 2018, DOI:10.1002/anie.201813174.